PHYSICAL REVIEW C VOLUME 24, NUMBER 4 OCTOBER 1981

# Low-lying spectra of transitional odd-mass nuclei described in angular momentum projected one-quasiparticle states

Akitsu Ikeda
*Department of Physics, Tokyo Institute of Technology, Oh-okayama, Meguro, Tokyo*
(Received 7 November 1980)

A previously proposed model of a particle coupled to a soft rotor is extended in order that both of the unique parity and the normal parity orbits can be indiscriminately treated in the same framework. Numerical calculations are performed for the odd-mass La and Pd isotopes. The low-lying energy spectra and variation of the spectra with mass number are well reproduced.

[NUCLEAR STRUCTURE $^{127,129,131,133,135}$La, $^{101,103,105,107,109}$Pd; calculated levels, $J$, $\pi$. Approximate angular momentum projection out of one-quasiparticle states.]

## I. INTRODUCTION

During recent years, a great deal of experimental data of band structures of odd-mass nuclei have been accumulated.[1] Most of the band structures, except for the closed and nearly closed shell regions, have been successfully analyzed and understood in terms of the rotation aligned coupling (RAC) scheme. The RAC scheme plays an important role not only in odd-mass nuclei but also in backbending phenomena of even nuclei. Thus, the RAC scheme is one of the fundamental coupling schemes for low-lying nuclear states in various regions of the Periodic Table.

Restricting ourselves to odd-mass nuclei, there are two other well known coupling schemes, i.e., the Bohr-Mottelson strong coupling and the particle-core weak coupling schemes. In the former, the deformation of intrinsic states is of primary importance and the Coriolis force is treated as a small perturbation. In the latter, on the other hand, the core is implicitly assumed to be spherically symmetric. The RAC scheme is obviously different from them, but has specific relations to them. Under some circumstances, the Coriolis force becomes very strong, and then the strong coupling scheme is destroyed and undergoes a change into the RAC scheme.[2] On the other hand, the particle-core coupling scheme tends toward the RAC scheme as the deformation of the core, measured by the quadrupole moment, grows.[3] In view of these relations, we can say that not only the rotational excitation of the core but also its deformation felt by the odd nucleon are important ingredients in the realistic RAC scheme.

The typical RAC scheme is actually observed not in the well-deformed region but in the transitional region where the core is not represented well by a rigid rotor with an $I(I+1)$ spectrum. Several authors removed the rigid rotor assumption from their calculations by using various methods such as the variable moment of inertia (VMI) model.[4] Application of the angular momentum projection method to odd-mass nuclei was also proposed by Ikeda, Onishi, and Sheline.[5,6] A feature of their model is that the deformed intrinsic wave function of the core is represented by a coherent state of the quadrupole boson, which was introduced into the nuclear physics by Haapakoski *et al.*[7] to reproduce the quasirotational ground band of $^{152}$Sm and $^{152}$Gd. Recently, Ewart and de Takacsy[8] performed a microscopic calculation for even Ba isotopes using the idea of the coherent state. Without the use of the coherent state or any other possible approximations, the angular momentum projection method for the case of odd-mass nuclei would require too much numerical work to be a practical method. Raduta *et al.*[9] performed calculations similar to those of Ref. 5 by using the fourth-order boson Hamiltonian to obtain a better fit to higher spin states.

Although many theoretical works have been done to study the nuclear structure of transitional, odd-mass nuclei, almost all of them are concerned with only the levels in which the intruder orbits are involved. The other levels have not received as much attention in the framework of particle-rotor coupling models. This unbalanced theoretical development may be largely attributed to the fact that the whole problem becomes more complicated in the case of non-intruder orbits due to the Nilsson mixing, which can be ignored in the case of intruder orbits. However, we would expect that such levels can also be described in terms of

 

a coupled system of a soft rotor and a particle which moves in non-intruder orbits. It may happen that the particle-soft rotor coupling model does not result in the rotation aligned coupling scheme when non-intruder orbits are involved, because the Coriolis force may not be as strong as in the case of intruder orbits. Therefore a realistic and reliable calculation is required to predict the resultant energy spectra.

The main objective of the present paper is to use the particle-soft rotor coupling model in the angular momentum projection method to calculate not only the nuclear levels involving intruder orbits but also the ones in which a particle moves in non-intruder orbits. The formulation of the model will be presented in Sec. II. Results of numerical calculations will be presented in Sec. III. We will discuss the results in Sec. IV.

## II. FORMULATION OF THE MODEL

Numerical calculations in the angular momentum projection method, if performed without any approximation, would require too much computing time even for even nuclei. The calculation for odd-mass nuclei is usually more laborious than for even nuclei. This situation led to a few practical approximations such as a power series expansion of the kernels,[10] and a classical field approximation which utilized coherent states of the quadrupole boson.[7] Both of them were originally developed for even nuclei. Ring, Mang, and Banerjee[11] developed an approximate method to perform a variation-after-projection calculation for even as well as odd-mass nuclei. Their method is quite useful for well-deformed nuclei. Recently Hara and Iwasaki[12] have done exact calculations of angular momentum and number projection out of the BCS wave functions based on the Nilsson scheme for the unique parity states of the odd-mass Yb isotopes. The present model, on the other hand, is based on the use of the coherent boson model and intended to work for transitional as well as deformed odd-mass nuclei.

The total Hamiltonian of the system consists of three parts:

$$H = H_c + H_p + H_{\text{int}} . \tag{2.1}$$

The Hamiltonian $H_c$ is for the core and is written in terms of bosons of angular momentum 2 as follows

$$H_c = \sum_{n,n'} \sum_{\lambda\lambda' I} h^I_{nn'}(\lambda\lambda')[(b^{\dagger n})^{(\lambda I)} \cdot (b^{n'})^{(\lambda' I)}] , \tag{2.2}$$

where $n$ and $n'$ denote the number of creation and annihilation operators for bosons which couple to angular momentum $I$ with seniority $\lambda$ and $\lambda'$, respectively. A possible way to obtain the eigenstates of the Hamiltonian $H_c$ is to use coherent states to represent deformed intrinsic states:

$$|\xi\eta\rangle = \exp[-\tfrac{1}{2}\xi^2 + \xi\cos\eta\, b^\dagger_{20} + 2^{-1/2}\xi\sin\eta(b^\dagger_{22} + b^\dagger_{2-2})]|0\rangle . \tag{2.3}$$

The eigenstates can be obtained by superimposing the coherent states (2.3) over $\xi$ and $\eta$ with weight functions $f_{JK}(\xi\eta)$:

$$\Psi_{J\mu} = N_J \left(\frac{2J+1}{8\pi^2}\right)^{1/2} \sum_K \int \xi^2 d\xi \sin 3\eta d\eta f_{JK}(\xi\eta) \times \int d\Omega \mathfrak{D}^{J\dagger}_{K\mu}(\Omega)\hat{R}(\Omega)|\xi\eta\rangle ,$$

where $\Omega$ abbreviates the Euler angles $(\psi, \theta, \chi)$ and $\hat{R}(\Omega)$ is the rotation operator. The integration over the Euler angles is just the angular momentum projection. The weight function $f_{JK}(\xi\eta)$ can be determined by solving the Hill-Wheeler equation of the generator coordinate method. Useful approximations are obtained, especially for the description of soft rotor spectra, by taking only one intrinsic state. This intrinsic state is determined by minimizing the expectation value:

$$\langle \xi\eta | H_c | \xi\eta\rangle = U_2\xi^2 + U_3\xi^2\cos 3\eta + U_4\xi^4 + \cdots , \tag{2.4}$$

where $U$'s are functions of $h^I_{nn'}(\lambda\lambda')$ of (2.2). Terminating the boson Hamiltonian $H_c$ at the fourth order, i.e., $n+n' \leq 4$, we obtain the minimum of (2.4) at $\eta = 0$ and

$$\xi = [-3U_3 + (9U_2 - 32U_2U_4)^{1/2}]/8U_4$$

for $U_2 < 0$, $U_3 < 0$, and $U_4 > 0$. Then the overlap and energy kernels turn out to be

$$\langle \xi | \hat{R}(\Omega) | \xi\rangle = \exp\{\xi^2[-1 + P_2(\cos\theta)]\}$$

and

$$\langle \xi | H_c \hat{R}(\Omega) | \xi\rangle / \langle \xi | \hat{R}(\Omega) | \xi\rangle = c_0 + c_2 P_2(\cos\theta) + c_4 P_4(\cos\theta) ,$$

where

$$|\xi\rangle \equiv |\xi,\ \eta = 0\rangle = \exp[-\tfrac{1}{2}\xi^2 + \xi b^\dagger_{20}]|0\rangle . \tag{2.5}$$

Consequently, the rotational spectrum of the even system is parametrized with the three parameters $\xi$, $c_2$, and $c_4$. The parameter $c_4$ affects the energy spectra only for high-spin states. Since we are interested in the energy spectra of states in the odd system which do not have high spins and which consequently do not involve very high spin states ($J \gtrsim 10$) of the even core, we put $c_4 = 0$.

In order to introduce single particle degrees of freedom, we have to fix the relation of the intrinsic state of the even core (2.5) to single particle operators. This is done by regarding the coherent state (2.5) as a deformed BCS vacuum, i.e.,

$$\alpha_{\sigma K}|\xi\rangle = 0\,, \tag{2.6}$$

where $\alpha_{\sigma K}$ ($\alpha^{\dagger}_{\sigma K}$) are annihilation (creation) operators of the BCS quasiparticle specified by the symmetry axis component of angular momentum $K$ and other quantum numbers $\sigma$.

The second term of (2.1) is

$$H_p = \sum (\epsilon_j - \lambda) c^{\dagger}_{jm} c_{jm} - \frac{G}{4} \sum c^{\dagger}_{jm} c^{\dagger}_{j\tilde{m}} c_{j'\tilde{m}'} c_{j'm'}\,, \tag{2.7}$$

where $\epsilon_j - \lambda$ are the spherical shell model single particle energies relative to the Fermi level, $G$ is the pairing interaction strength, and $(j\tilde{m})$ denotes the time reversed state of $(jm)$. A very simple form is assumed for the interaction Hamiltonian:

$$H_{\rm int} = \sum_{\nu} [b_{2\nu} + (-1)^{\nu} b^{\dagger}_{2-\nu}] q_{\nu}\,. \tag{2.8a}$$

with

$$q_{\nu} = \sum_{\alpha,\beta} \langle \alpha | V(r) Y_{2\nu}(\theta\psi) | \beta \rangle c^{\dagger}_{\alpha} c_{\beta}\,. \tag{2.8b}$$

The following form is adopted for $V(r)$:

$$V(r) = kr^2\,. \tag{2.9}$$

The deformed BCS scheme mentioned above is obtained as follows. First, $H_{\rm int}$ is averaged over the intrinsic state of the core (2.5), giving rise to a deformed field

$$\langle \xi | H_{\rm int} | \xi \rangle = 2k\xi \sum_{\alpha,\beta} \langle \alpha | r^2 Y_{20}(\theta\psi) | \beta \rangle c^{\dagger}_{\alpha} c_{\beta}\,, \tag{2.10}$$

where only the $Y_{20}$ term survives because axial symmetry has been assumed in (2.5). Then we diagonalize the single particle energy term of $H_p$ plus the deformed field (2.10), which is nothing but the Nilsson model, to obtain deformed orbits $(\sigma K)$

$$c_{\sigma K} = \sum_{j} W^{\sigma K}_{j} c_{jK}\,, \tag{2.11}$$

where $W^{\sigma K}_{j}$ are Nilsson coefficients. Then we apply the BCS presciption to

$$H_p + \langle \xi | H_{\rm int} | \xi \rangle = \sum \epsilon_{\sigma K} c^{\dagger}_{\sigma K} c_{\sigma K} - \tfrac{1}{4} G \sum c^{\dagger}_{\sigma K} c^{\dagger}_{\sigma\tilde{K}} c_{\sigma'\tilde{K}'} c_{\sigma' K'}$$

to define the deformed BCS quasiparticles

$$\alpha^{\dagger}_{\sigma K} = u_{\sigma K} c^{\dagger}_{\sigma K} - v_{\sigma K} c_{\sigma\tilde{K}}\,, \tag{2.12}$$

where $u$'s and $v$'s are the Bogoliubov transformation coefficients. Only the one-quasiparticle states are employed in the present paper as the intrinsic states, out of which basis functions are projected:

$$|IM\sigma K\rangle = n^{I}_{\sigma K} \left(\frac{2I+1}{8\pi^2}\right)^{1/2} \int d\Omega \mathfrak{D}^{I\,\dagger}_{KM}(\Omega) \hat{R}(\Omega) \alpha^{\dagger}_{\sigma K} |\xi\rangle\,. \tag{2.13}$$

The Hamiltonian (2.1) is diagonalized in the space spanned by the projected wave functions (2.13). The basis functions are not orthogonal to each other, and we need to simultaneously diagonalize the Hamiltonian and overlap matrices.

Denoting by $\hat{O}$ a $c$ number or a scalar composed of fermion and/or boson operators, the overlap and Hamiltonian matrix elements are of the form

$$\langle IM, \sigma_1 K_1 | \hat{O} | IM, \sigma_2 K_2 \rangle = n^{I}_{\sigma_1 K_1} n^{I}_{\sigma_2 K_2} \int d\Omega \mathfrak{D}^{I*}_{K_1 K_2}(\Omega) h_{\sigma_1 K_1, \sigma_2 K_2}(\hat{O}; \Omega)\,, \tag{2.14}$$

where

$$h_{\sigma_1 K_1, \sigma_2 K_2}(\hat{O}; \Omega) \equiv \langle \xi | \alpha_{\sigma_1 K_1} \hat{O} \hat{R}(\Omega) \alpha^{\dagger}_{\sigma_2 K_2} | \xi \rangle \tag{2.15a}$$

$$= \langle \xi | \alpha_{\sigma_1 K_1} \hat{R}(\Omega) \hat{O} \alpha^{\dagger}_{\sigma_2 K_2} | \xi \rangle\,. \tag{2.15b}$$

The transformation property of quasiparticle operators $\alpha^{\dagger}$ and $\alpha$ is found by expanding them in terms of the spherical shell model basis functions,

$$\hat{R}(\Omega) \alpha^{\dagger}_{\sigma K} \hat{R}(\Omega)^{-1} \equiv \alpha^{\dagger}_{\sigma K}[\Omega] = \sum_{j} W^{\sigma K}_{j} \sum_{m} \mathfrak{D}^{j}_{mK}(\Omega) (u_{\sigma K} c^{\dagger}_{jm} - v_{\sigma K} c_{j\tilde{m}})\,. \tag{2.16}$$

We calculate $h_{\sigma_1 K_1, \sigma_2 K_2}(\hat{O}; \Omega)$ in an approximate way. Substituting $\hat{O} = 1$ in Eq. (2.15) and making use of Eq. (2.16), we obtain for the overlap matrix

$$h_{\sigma_1 K_1, \sigma_2 K_2}(1; \Omega) = \langle \xi | [A^{(0)}_{\sigma_1 K_1, \sigma_2 K_2}(\Omega) + A^{(2)}_{\sigma_1 K_1, \sigma_2 K_2}(\Omega)] \hat{R}(\Omega) | \xi \rangle\,, \tag{2.17}$$

where $A^{(0)}$ and $A^{(2)}$ stand for zero- and two-quasiparticle configurations, respectively,

$$A^{(0)}_{\sigma_1 K_1, \sigma_2 K_2}(\Omega) = \sum_{j} W^{\sigma_1 K_1}_{j} \mathfrak{D}^{j}_{K_1 K_2}(\Omega) W^{\sigma_2 K_2}_{j} \times (u_{\sigma_1 K_1} u_{\sigma_2 K_2} + v_{\sigma_1 K_1} v_{\sigma_2 K_2}) \tag{2.18}$$

and

$$A^{(2)}_{\sigma_1 K_1, \sigma_2 K_2}(\Omega) = \sum_{\sigma, K} \alpha_{\sigma_1 K_1} \alpha_{\sigma K} (v_{\sigma K} u_{\sigma_2 K_2} - u_{\sigma K} v_{\sigma_2 K_2}) \times \sum_{j} W^{\sigma K}_{j} \mathfrak{D}^{j}_{K K_2}(\Omega) W^{\sigma_2 K_2}_{j}\,. \tag{2.19}$$

The $A^{(2)}$ term of $h(1; \Omega)$ obviously vanishes when $(\psi, \theta, \chi) = (\psi, 0, \chi)$ and, therefore, its contribution

to the integral of Eq. (2.14) is expected to be small as long as $\theta$ remains small. Its contribution to the integral from rather large values of $\theta$ can be expected to be suppressed as much as that of the $A^{(0)}$ term owing to the overlap function, which is a rapidly decreasing function of $\theta$ [see (2.21)]. In addition to the different angular dependence of the two terms, the factor $(uv-uv)$ makes the $A^{(2)}$ term less important than the $A^{(0)}$ term which has $(uu+vv)$ instead. Based on these considerations, we approximately calculate $h(1;\Omega)$ by retaining only the $A^{(0)}$ term. Then it is factorized into the odd particle part and the core overlap $n(\Omega)$,

$$h_{\sigma_1 K_1,\sigma_2 K_2}(1;\Omega)\approx\left[\sum_j W^{\sigma_1 K_1}_j \mathfrak{D}^j_{K_1 K_2}(\Omega) W^{\sigma_2 K_2}_j (u_{\sigma_1 K_1}u_{\sigma_2 K_2}+v_{\sigma_1 K_1}v_{\sigma_2 K_2})\right] n(\Omega)\,, \tag{2.20}$$

with

$$n(\Omega)\equiv\langle\xi|\hat{R}(\Omega)|\xi\rangle=\exp[-\xi^2+\xi^2\mathfrak{D}_{00}{}^2(\Omega)]\,. \tag{2.21}$$

Other matrix elements can be calculated consistently with $h(1;\Omega)$ using the following approximation:

$$\langle\xi|\alpha_{\sigma_1 K_1}\hat{O}_F\hat{R}(\Omega)\alpha^\dagger_{\sigma_2 K_2}|\xi\rangle = \langle\xi|\alpha_{\sigma_1 K_1}\hat{O}_F\alpha^\dagger_{\sigma_2 K_2}[\Omega]\hat{R}(\Omega)|\xi\rangle - \langle\xi|\alpha_{\sigma_1 K_1}\hat{O}_F\alpha^\dagger_{\sigma_2 K_2}[\Omega]|\xi\rangle\langle\xi|\hat{R}(\Omega)|\xi\rangle \tag{2.22a}$$

or

$$-\langle\xi|\alpha_{\sigma_1 K_1}[\Omega]\hat{O}_F\alpha^\dagger_{\sigma_2 K_2}|\xi\rangle\langle\xi|\hat{R}(\Omega)|\xi\rangle\,, \tag{2.22b}$$

where $\hat{O}_F$ is understood not to contain boson operators. Applying the approximation (2.22a) to $H_p$, we obtain

$$h_{\sigma_1 K_1,\sigma_2 K_2}(H_p;\Omega)=\xi\sum_\tau\left\{\left[\sum_j(\epsilon_j-\lambda)W^{\sigma_1 K_1}_j W^{\tau K_1}_j\right](u_{\sigma_1 K_1}u_{\tau K_1}-v_{\sigma_1 K_1}v_{\tau K_1}) + \delta_{\tau_1\sigma_1}[2\Delta u_{\sigma_1 K_1}v_{\sigma_1 K_1}-G(u_{\sigma_1 K_1}{}^2-v_{\sigma_1 K_1}{}^2)v_{\sigma_1 K_1}{}^2]\right\}h_{\tau K_1,\sigma_2 K_2}(1;\Omega)\,, \tag{2.23}$$

where $\Delta$ denotes the pairing gap energy.

This expression appears to be asymmetric with respect to the indices, but it can be seen that it conserves Hermiticity in a representation in which the overlap matrix is a unit matrix. When $O$ contains boson operators as $H_c$ and $H_{\rm int}$, we operate first the boson operators on $|\xi\rangle$ or on $\langle\xi|$ and replace them with $c$ numbers by using a simple property of the coherent state

$$b_{2\nu}e^{\sum\alpha_\mu b^\dagger_{2\mu}}|0\rangle=\alpha_\nu e^{\sum\alpha_\mu b^\dagger_{2\mu}}|0\rangle\,.$$

Applying this procedure to $H_c$ and $H_{\rm int}$, we obtain

$$h_{\sigma_1 K_1,\sigma_2 K_2}(H_c;\Omega)=c\xi^2\mathfrak{D}_{00}{}^2(\Omega)\langle\xi|\alpha_{\sigma_1 K_1}\alpha^\dagger_{\sigma_2 K_2}[\Omega]\hat{R}(\Omega)|\xi\rangle \tag{2.24}$$

and

$$h_{\sigma_1 K_1,\sigma_2 K_2}(H_{\rm int};\Omega)=\xi\{\langle\xi|\alpha_{\sigma_1 K_1}q_{\mu=0}\alpha^\dagger_{\sigma_2 K_2}[\Omega]\hat{R}(\Omega)|\xi\rangle+\langle\xi|\hat{R}(\Omega)\alpha_{\sigma_1 K_1}[\Omega]q_{\mu=0}\alpha^\dagger_{\sigma_2 K_2}|\xi\rangle\}\,. \tag{2.25}$$

Applying the approximations (2.17) to the above expectation values, we obtain

$$h_{\sigma_1 K_1,\sigma_2 K_2}(H_c;\Omega)=c\xi^2\mathfrak{D}_{00}{}^2(\Omega)\cdot h_{\sigma_1 K_1,\sigma_2 K_2}(1;\Omega)\,, \tag{2.24'}$$

and

$$h_{\sigma_1 K_1,\sigma_2 K_2}(H_{\rm int};\Omega)=\xi\sum_\tau[h_{\sigma_1 K_1,\tau K_2}(1;\Omega)\langle\tau K_2|V(r)Y_{20}|\sigma_2 K_2\rangle(u_{\tau K_2}u_{\sigma_2 K_2}-v_{\tau K_2}v_{\sigma_2 K_2}) + \langle\sigma_1 K_1|V(r)Y_{20}|\tau K_1\rangle(u_{\sigma_1 K_1}u_{\tau K_1}-v_{\sigma_1 K_1}v_{\tau K_1})h_{\tau K_1,\sigma_2 K_2}(1;\Omega)]\,. \tag{2.25'}$$

We can now calculate the Hamiltonian and the overlap matrices by substituting expressions (2.20), (2.23), (2.24′), and (2.25′) into (2.14).

The present model contains three phenomenological parameters $\xi$, $c_2$, and $k$ in addition to single particle energies $\epsilon_j$ and the pairing strength $G$. The first two parameters determine the properties of the even core: $\xi$ fixes the spectral pattern and $c_2$ works as an energy scale. We can roughly estimate them by approximately reproducing the yrast band of the adjacent even nuclei. An approximate estimation of $k$ can be obtained by equating expression (2.10) to the Nilsson potential

$$2k\xi=-0.95\beta\omega\,, \tag{2.26}$$

where the deformation $\beta$ can be evaluated using Grodzins's empirical formula. We perform numerical calculations by varying the parameters around

the values estimated above for a better fit to the experimental data. Deviation of the parameters by a few tens percent from the starting values is considered to be acceptable.

## III. APPLICATION TO THE Pd AND La ISOTOPES

In order to fix the single particle energy term of $H_{pt}$ we use the harmonic oscillator model with the $[\vec{l}^2 - \langle \vec{l}^2 \rangle_N]$ and $l \cdot s$ terms included, which is just the Nilsson Hamiltonian in the spherical limit specified by coefficients $\mu$ and $\kappa$. Several sets of $(\mu, \kappa)$ values have been proposed in the course of energy surface calculations[13-16] and spectroscopic studies[17,18] in these mass regions. It is found that all of them, when used in the present model, yield the characteristic features such as the $\frac{11}{2}^-$, $\frac{7}{2}^+$, and $\frac{5}{2}^+$ $\Delta I = 2$ bands in the Pd isotopes, but that the bandhead energies are rather strongly influenced by the set used. From the overall quality of agreement between experiment and theory, particular sets of $(\mu, \kappa)$ values with certain modifications are selected for the Pd and La isotopes (see Table I). The present single particle energies are similar to the ones of Refs. 14, 16, and 17.

### A. The Pd isotopes

One of the characteristic features of the odd-$A$ Pd isotopes is that all the ground states from $^{101}\mathrm{Pd}_{55}$ to $^{109}\mathrm{Pd}_{63}$ are $\frac{5}{2}^+$ and have fairly strong single particle strength.[19] This is very difficult to understand in the spherical shell model or in the quasiparticle-vibrator coupling model, if either one of $2d_{5/2}$ or $1g_{7/2}$ is once assumed to be lower than the other for all the Pd isotopes. The Purdue group[20] discovered $\frac{11}{2}^-$, $\frac{7}{2}^+$, and $\frac{5}{2}^+$ bands in $^{101,103,105}$Pd. $\frac{5}{2}^+$ bands in $^{101,103}$Pd and $\frac{11}{2}^-$ and $\frac{7}{2}^+$ bands in all three nuclides are decoupled $\Delta I = 2$ bands, whereas the $\frac{5}{2}^+$ band in $^{105}$Pd looks like a very perturbed rotational $\Delta I = 1$ band. Klarma and Rekstad[21] found in $^{107}$Pd a $\frac{7}{2}^+$ level, which is strongly connected to the ground state, and decoupled $\frac{11}{2}^-$ and $\frac{7}{2}^+$ bands using the $(\alpha, n\gamma)$ reaction.

TABLE I. The values of $\mu$, $\kappa$ adopted in the present calculation and additional energy shifts for several orbits.

| | | | Energy shifts in the unit of $(\hbar\omega_0)$ |
|---|---|---|---|
| Pd | $\mu_n$ $(N=4)$ | 0.35 | −0.10 for $3s_{1/2}$, $2d_{3/2}$, $2d_{5/2}$ |
| | $\kappa_n$ $(N=4)$ | 0.0637 | 0.13 for $1g_{7/2}$ |
| | $\mu_n$ $(N=5)$ | 0.42 | 0.13 for $1h_{11/2}$ |
| | $\kappa_n$ $(N=5)$ | 0.0637 | |
| La | $\mu_p$ $(N=4)$ | 0.6 | −0.08 for $2d_{3/2}$ |
| | $\kappa_p$ $(N=4)$ | 0.0637 | −0.03 for $1g_{7/2}$ |
| | $\mu_p$ $(N=5)$ | 0.6 | 0.10 for $1h_{11/2}$ |
| | $\kappa_p$ $(N=5)$ | 0.0637 | |

TABLE II. The values of parameters used in the present calculation. $\beta$ determines the strength of the particle-core coupling through Eq. (2.26). The following pairing strengths are used: $G_n = 22.5/A$ (for Pd) and $G_p = 17.0/A$ (for La).

| | $\xi$ | $c_2\xi^{-2}$ (MeV) | $\beta$ |
|---|---|---|---|
| $^{101}$Pd | 1.72 | 1.16 | 0.195 |
| $^{103}$Pd | 1.87 | 1.19 | 0.214 |
| $^{105}$Pd | 1.93 | 1.23 | 0.224 |
| $^{107}$Pd | 1.92 | 1.20 | 0.225 |
| $^{109}$Pd | 1.95 | 1.07 | 0.246 |
| $^{127}$La | 2.35 | 1.06 | 0.195 |
| $^{129}$La | 2.28 | 1.05 | 0.183 |
| $^{131}$La | 2.10 | 1.09 | 0.155 |
| $^{133}$La | 2.02 | 1.26 | 0.133 |
| $^{135}$La | 1.88 | 1.37 | 0.113 |

Numerical calculations were carried out in the present model for these nuclei. Values of the parameters are listed in Table II. Variations of the lowest levels of each spin value with mass number are shown in Fig. 1. It is remarkable that the correct spin value is obtained for all the ground states from $^{101}$Pd to $^{109}$Pd. In the spherical shell model an increase of the number of particles results in the monotonic filling of successive orbits, but in the present model particles are distributed over various orbits because of the deformation and the pairing correlations, and the $d_{5/2}$ orbital remains partially empty throughout the isotopes investigated. Actually, $\frac{5}{2}^+[422]$ stays very close to the Fermi level from $^{101}$Pd to $^{109}$Pd and this is the reason $\frac{5}{2}^+$ remains as the ground state for all these nuclei. The variation of the $\frac{11}{2}^-$ bandhead energy with the mass number is also well reproduced. However, our calculations predict the $\frac{7}{2}^+$ states slightly too low in all the nuclei, and we are not successful in describing the behavior of the lowest $\frac{3}{2}^+$ levels. It may be worth noting that any shift in the single particle energy of $d_{3/2}$ does not improve the situation. The calculated and experimental energy spectra of $^{101}$Pd, $^{103}$Pd, and $^{105}$Pd are illustrated in Figs. 2–4. The illustrated experimental data are consistent with the adopted levels of the Nuclear Data Sheets.[22] Those levels which are observed to constitute bands in in-beam experiments are shown separately from the others. The calculated levels are also classified into those which constitute bands and those which do not. The classification is easily done by investigating the structure of the wave functions.

The calculated $\frac{11}{2}^-$ bands in Figs. 2(b), 3(b), and

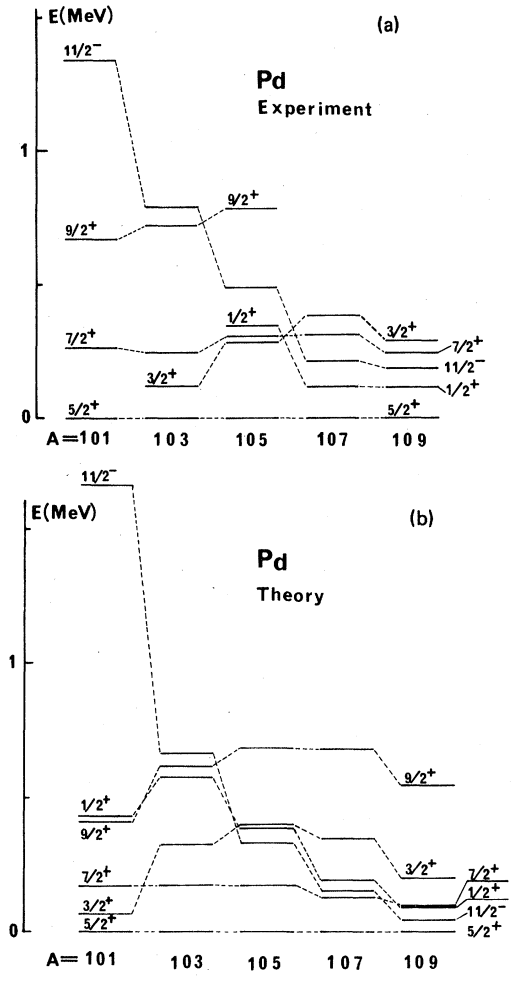


FIG. 1. Variation of the lowest states of $\frac{1}{2}^+ \sim \frac{9}{2}^+$ and $\frac{11}{2}^-$ with mass number for the odd mass Pd isotopes. (a) Theoretical results and (b) experimental data. Twice the spin value is noted instead of $J$ itself.

4(b) are just the $h_{11/2}$ decoupled band as expected. Actually the parameters $c$ and $\xi$ are adjusted to reproduce the $\frac{15}{2}^- - \frac{11}{2}^-$ energy difference and the ratio $[E(\frac{19}{2}^-) - E(\frac{15}{2}^-)]/[E(\frac{15}{2}^-) - E(\frac{11}{2}^-)]$. It is a success of the present model that the excitation energy of the $\frac{7}{2}^-$ level relative to the $\frac{11}{2}^-$ is obtained correctly in $^{105}$Pd and probably in $^{103}$Pd. The calculated $\frac{5}{2}^+$ ground bands from $^{101}$Pd to $^{105}$Pd are essentially the $d_{5/2}$ decoupled band and compare very well with the experimental data. It should be noted, however, that the calculated $\frac{9}{2}^+ - \frac{5}{2}^+$ energy difference is slightly too small in all three isotopes. This energy difference is most strongly influenced by the parameter $c$. However, this parameter has already been fixed as described above. In the calculated $\frac{7}{2}^+$ bands starting at 0.169, 0.172, and 0.172 MeV in $^{101}$Pd, $^{103}$Pd, and $^{105}$Pd, respectively, the $g_{7/2}$ orbital is dominantly involved. These bands can be identified with the $g_{7/2}$ decoupled band. They correspond very well to the experimental data. We obtain another $\frac{7}{2}^+$ band in $^{103}$Pd and $^{105}$Pd starting at 0.482 and 0.452 MeV, respectively. They are characterized by strong involvement of $d_{5/2}$ and can be identified with the unfavored $d_{5/2}$ decoupled band. In $^{101}$Pd, the $\frac{7}{2}^+$ state at 0.702 MeV and the $\frac{11}{2}$ state at 1.533 MeV have similar character but we cannot trace to higher spin levels because of heavy mixing. The "unfavored" $\frac{7}{2}^+$ band compares well with the experimental data in $^{105}$Pd where the $\frac{5}{2}^+$, $\Delta I = 2$ ground band and the $\frac{7}{2}^+$, $\Delta I = 2$ band taken together appear to constitute a $\Delta I = 1$ rotational-like band. We are not totally successful here, however, because the calculated $\frac{7}{2}^+$ $\Delta I = 2$ sequence grows faster in energy than the $\frac{5}{2}^+$ $\Delta I = 2$ sequence, in disagreement with the experimental data. In $^{103}$Pd, the $\frac{7}{2}^+$ unfavored band seems to correspond to the experimental levels with spins $\frac{7}{2}^+$ at 531.8 keV and $\frac{11}{2}^+$ at 1329.1 keV.

### B. The La isotopes

As is well known, the unique parity decoupled bands were observed for the first time in $^{125\text{-}137}$La using (heavy ion, $xn\gamma$) reactions.[23] Chiba[24] *et al.* performed in-beam experiments using rather light projectiles of comparatively low energies and succeeded in locating two nonunique parity $\Delta I = 2$ bands in $^{131,133}$La. Similar experiments were done recently on $^{133}$La by Morek[25] *et al.* with higher incident energies, and the level scheme has been extended to higher spins. A third $\Delta I = 2$ positive parity band starting at 88 keV with spin $\frac{5}{2}^+$ has been found. The latter authors also found some unfavored states, with spins $\frac{13}{2}^-$ and $\frac{17}{2}^-$, which have different positions than those proposed by Chiba *et al.* In contrast to the Pd isotopes, the last odd nucleon is the proton in the odd La isotopes, and obviously the number of protons does not vary throughout the isotopes. Therefore, the variation of level structure from one isotope to another comes primarily from the change of the number of neutrons, which is taken into account in the present model by the phenomenological parameters describing the core. The variations of the experimental and calculated lowest states of each spin with the mass number is shown in Figs. 5(a) and (b). The increase of the energy difference between the $\frac{11}{2}^-$ and $\frac{5}{2}^+$ states with the mass number has been reproduced well in the calculation. The $\frac{7}{2}^+$ and $\frac{5}{2}^+$ states behave similarly with respect to the $\frac{11}{2}^-$ states and are described well by our calculations, although the order of the $\frac{5}{2}^+$ and $\frac{7}{2}^+$ states is reversed in $^{131}$La. It should be

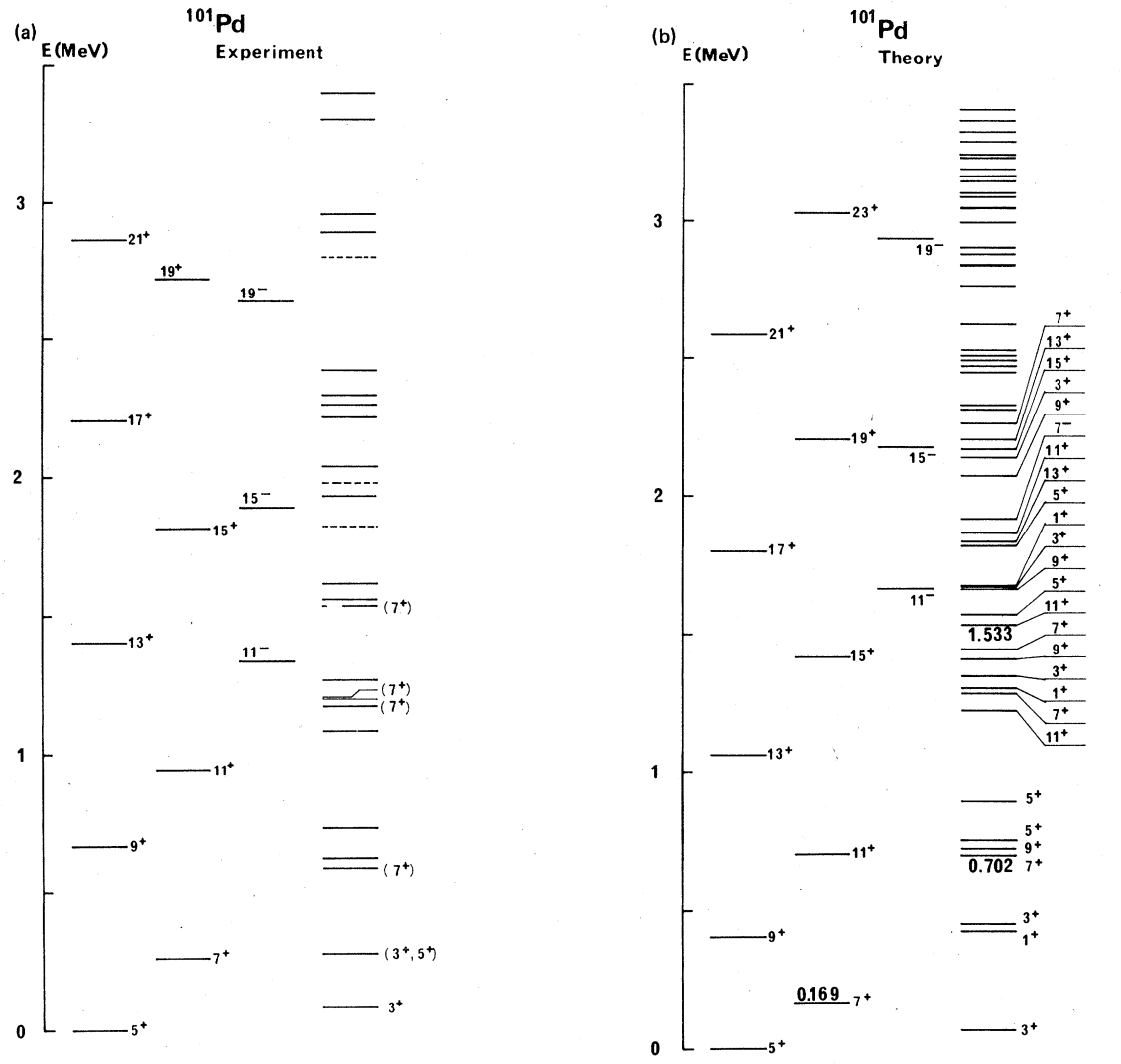


FIG. 2. Comparison between (a) theoretical and (b) experimental energy spectra of $^{101}$Pd. The levels which constitute a band are separately drawn from the others.

noted that this agreement is not brought about through shifts of single particle orbits from one isotope to another. The experimental excitation energies of the lowest $\frac{3}{2}^+$ states become lower in lighter isotopes and the $\frac{3}{2}^+$ states become the ground states of $^{129,131}$La. This behavior is not reproduced in the present calculation. Any shift of $d_{3/2}$ single particle energy does not improve the situation as in the Pd case. There is not sufficient experimental data on the lowest $\frac{1}{2}^+$ states to compare with the calculation. The experimental and calculated energy spectra of $^{133}$La are shown in Figs. 6(a) and (b). There are four distinct $\Delta I=2$ sequences in the calculated spectra. In the $\frac{5}{2}^+$ ground band $d_{5/2}$ is predominantly involved and can be identified with the $d_{5/2}$ decoupled band. This band compares well with the experimental data. The calculated $\frac{7}{2}^+$ and $\frac{9}{2}^+$ bands are made up of $g_{7/2}$ particle and core excitations, and can be identified with the favored and unfavored decoupled bands of $g_{7/2}$. There is a good agreement between theory and experiment with respect to the $\frac{7}{2}^+$ band. There is also a good correspondence between the calculated $\frac{9}{2}^+$ band and the $\frac{9}{2}^+$, $(\frac{13}{2}^+)$, and $(\frac{17}{2}^+)$ levels of the experimental $\frac{5}{2}^+$ band.

## IV. SUMMARY AND DISCUSSION

The point of the model proposed in this paper is that both the unique parity and the normal parity

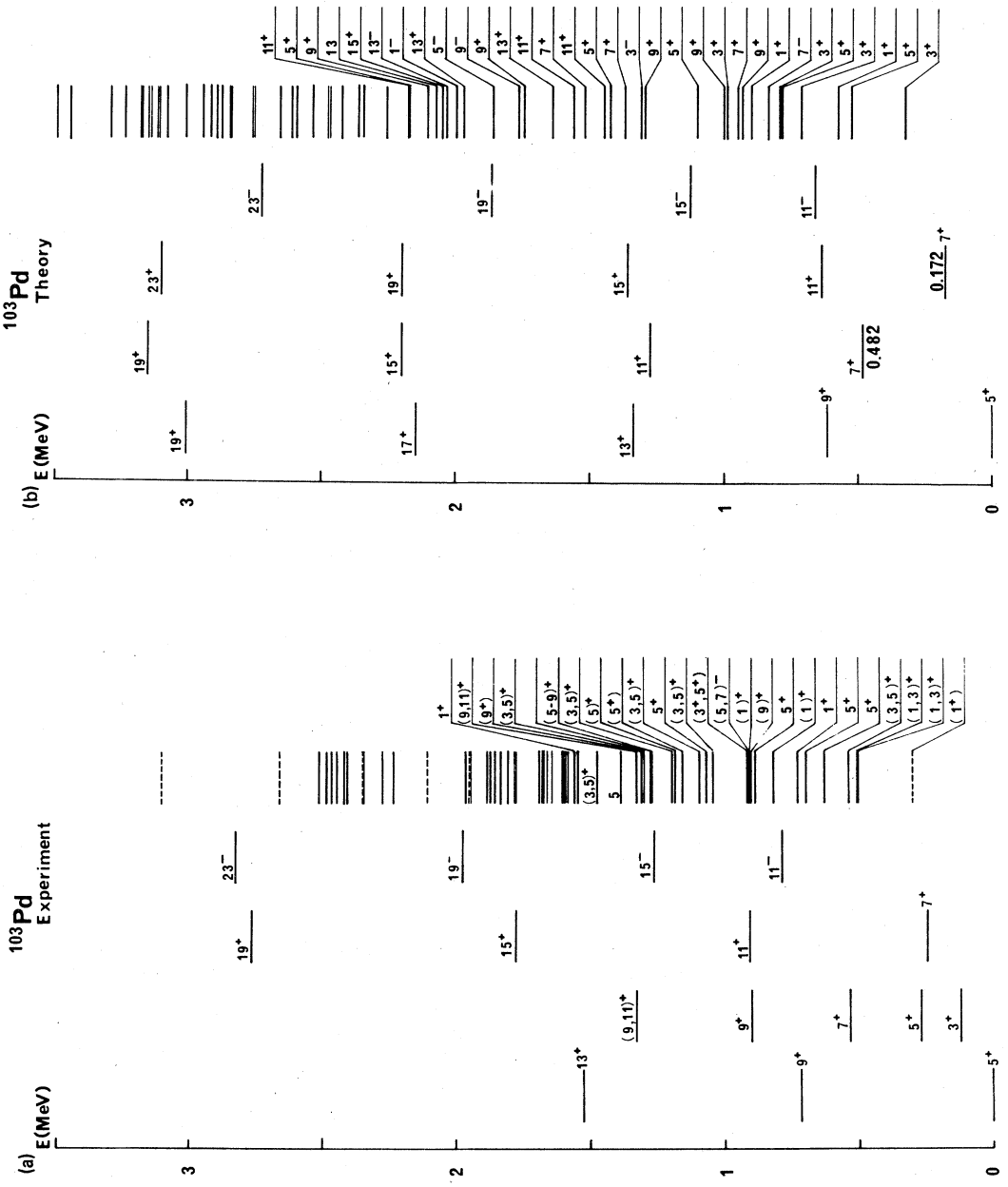


FIG. 3. Comparison between (a) theoretical and (b) experimental energy spectra of $^{103}$Pd. The levels which constitute a band are separately drawn from the others.

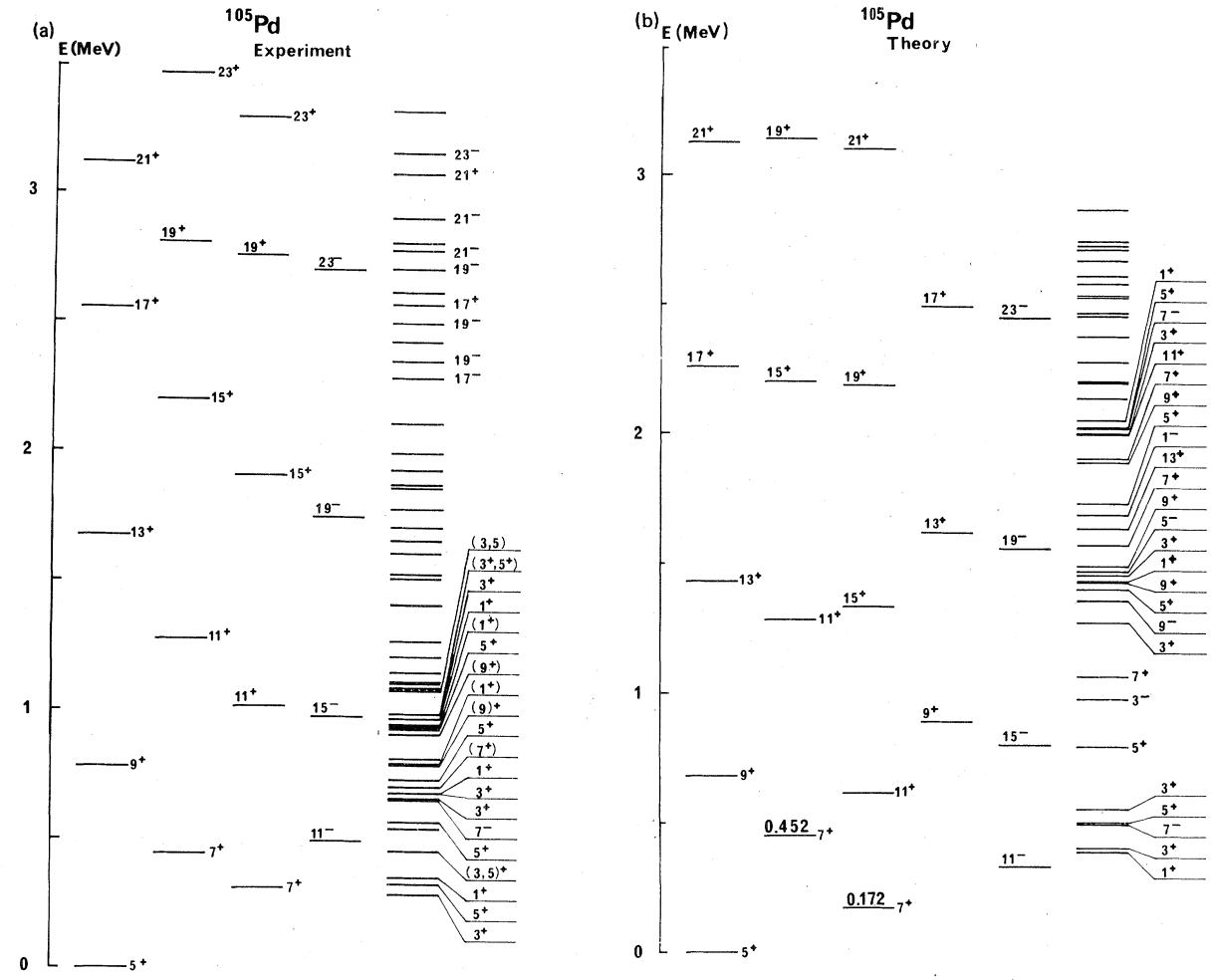


FIG. 4. Comparison between (a) theoretical and (b) experimental energy spectra of $^{105}$Pd. The levels which constitute a band are separately drawn from the others.

states are treated in a framework which is suitable for describing the rotation alignment. The model can be regarded as an approximate angular momentum projection method out of axially symmetric, weakly deformed one-quasiparticle states. The approximation is made through the use of the coherent boson states for the even core. The closure approximation, (2.22a) and (2.22b), is used to evaluate the overlap and the energy kernels. Our model can be characterized by the nonrigid rotational excitation of the core and an explicit incorporation of the deformation which defines realistic single particle orbitals. The present numerical calculation has given the following good results:

(1) In addition to the $\frac{11}{2}^-$ decoupled bands, the $\frac{7}{2}^+$, $\Delta I=2$ bands observed in $^{101,103,105}$Pd are all reproduced as the decoupled bands based on the $g_{7/2}$ orbital.

(2) All the $\frac{5}{2}^+$ bands observed in $^{101,103,105}$Pd are described very well. Especially, the change of the $\frac{5}{2}^+$ band from $\Delta I=2$ to $\Delta I=1$ character at $^{103}$Pd is reproduced. It is explained as a lowering of the $d_{5/2}$ unfavored band relative to the $d_{5/2}$ favored band, which is caused by an increase of the particle number, and which leads to an alternate order of the levels belonging to the two bands. The same applies to $^{133}$La, where the $\frac{7}{2}^+$, $\Delta I=2$ band and the $\frac{9}{2}^+$, $\Delta I=2$ band taken together constitute a $\Delta I=1$ rotational-like band.

(3) The correct spin and parity, $\frac{5}{2}^+$, is obtained for all the ground states of $^{101\text{-}109}$Pd. The agree-

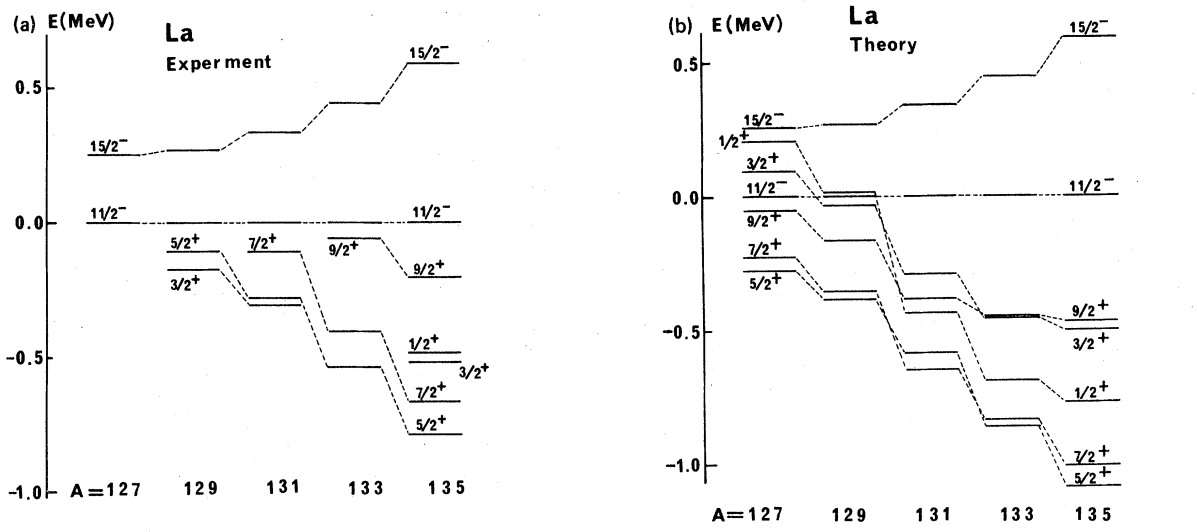


FIG. 5. Variation of the lowest states of $\frac{1}{2}^+ \sim \frac{9}{2}^+$, $\frac{11}{2}^-$, and $\frac{15}{2}^-$ with mass number for the odd mass La isotopes. (a) Theoretical results and (b) experimental data.

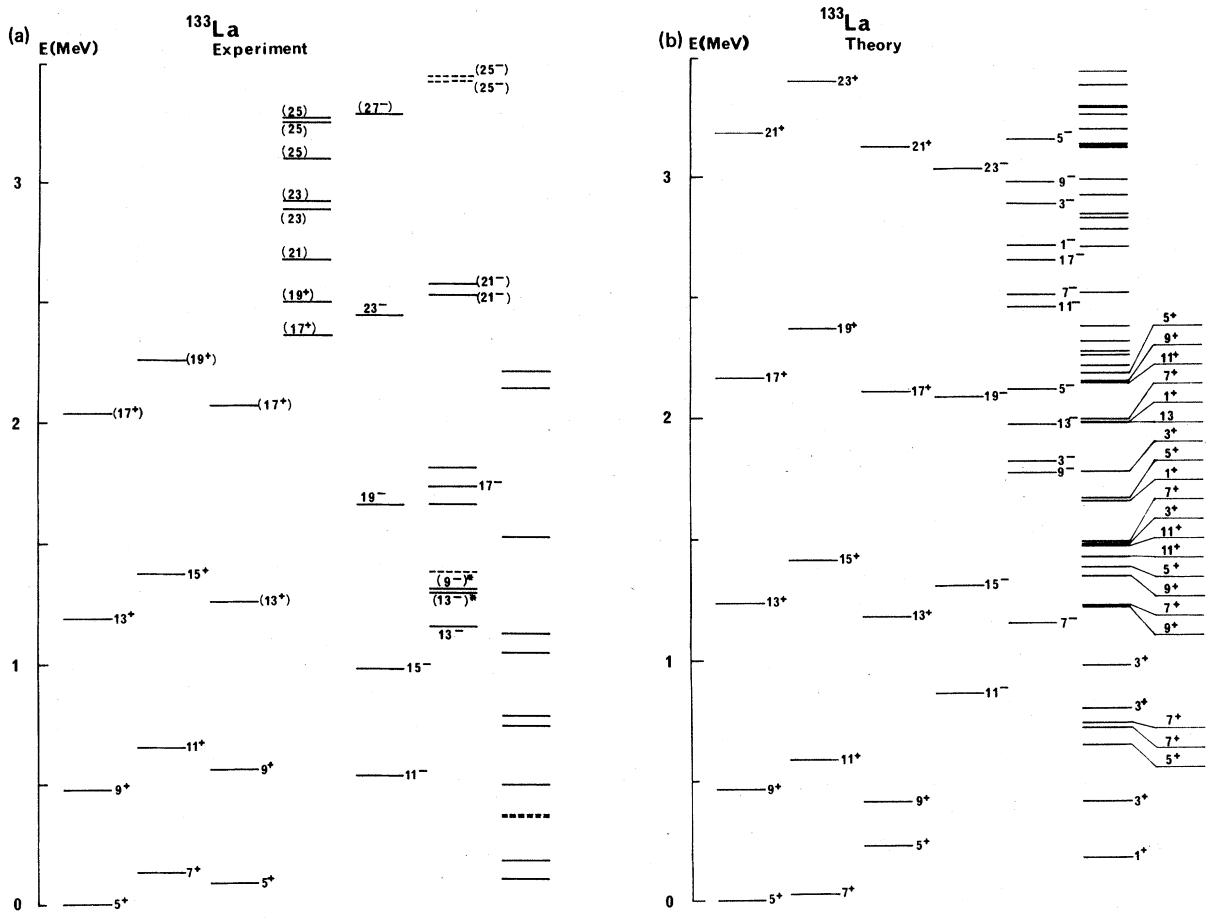


FIG. 6. Comparison between (a) theoretical and (b) experimental energy spectra of $^{133}$La. The experimental data are taken from Refs. 25 and 26. The levels marked with an asterisk are from Ref. 24.

ment is achieved with a proper location of the Fermi level in the deformed single particle spectrum, which changes from isotope to isotope as the deformation is varied consistently with the energy spectrum of the unique parity decoupled band. It gives strong support for the consistency of the present model.

(4) The variations of relative positions of the lowest $\frac{5}{2}^+$, $\frac{7}{2}^+$, and $\frac{11}{2}^-$ states with mass number is reproduced quite well both in the Pd and La isotopes.

The even Pd isotopes have long been considered to be typical vibrational nuclei. However, the present calculation shows that the explicit incorporation of deformation makes it possible to understand many features of the experimental energy spectra.

Some states with low spins, such as $\frac{3}{2}^+$ and $\frac{5}{2}^+$, at low excitation energies are not described well in the present calculation. In a recent $(n,\gamma)$ experiment[27] performed by Casten *et al.*, several low-spin, negative-parity states were found in $^{109}$Pd at low excitation energies, which the authors reported would not be described in terms of a simple rotation-aligned coupling scheme. The present calculation for $^{109}$Pd does not reproduce those low-spin negative-parity states either. Since our model has worked very well for the states with $I \geq j$, we can expect that the approximations used in the model do not break down for low-spin states either. Therefore the inability to describe the states with $I < j$ should be attributed not to the approximation but to an insufficiency of the model space. An attempt to include three-quasiparticle configurations in the model space is underway.

## ACKNOWLEDGMENTS

The computing facilities of University of Tokyo and Tokyo Institute of Technology were used for the calculation. The author is grateful to Prof. N. Onishi for valuable discussions. He thanks also Prof. S. Yoshida and Prof. T. T. Sugihara for their interest in this work.

[1]For a recent review, see R. M. Lieder and H. Ryde, Adv. Nucl. Phys. 10, 1 (1977).
[2]As a typical example, we refer to the positive parity bands of the odd mass Er isotopes. See Ref. 1.
[3]Y. Tanaka and R. K. Sheline, Phys. Lett. 58B, 414 (1975).
[4]H. Toki and A. Faessler, Nucl. Phys. A253, 231 (1975).
[5]A. Ikeda, R. K. Sheline, and N. Onishi, Phys. Lett. 44B, 39 (1973).
[6]A. Ikeda, N. Onishi, and R. K. Sheline, Prog. Theor. Phys. 56, 570 (1976).
[7]P. Haapakoski, P. Honkaranta, and P. O. Lipas, Phys. Lett. 31B, 493 (1970).
[8]G. M. Ewart and N. de Takacsy, Phys. Rev. C 17, 303 (1978).
[9]A. A. Raduta, V. Ceausescu, and R. M. Dreizler, Nucl. Phys. A272, 11 (1976).
[10]N. Onishi, R. K. Sheline, and S. Yoshida, Phys. Rev. C 2, 1304 (1970).
[11]P. Ring, H. J. Mang, and B. Banerjee, Nucl. Phys. A225, 141 (1974).
[12]K. Hara and S. Iwasaki, Nucl. Phys. A348, 200 (1980).
[13]Inger-Lena Lamm, Nucl. Phys. A125, 504 (1969).
[14]D. A. Arseniev, A. Sobiczewski, and V. G. Soloviev, Nucl. Phys. A126, 15 (1969).
[15]D. A. Arseniev, A. Sobiczewski, and V. G. Soloviev, Nucl. Phys. A139, 269 (1969).
[16]Lukasiak and A. Sobiczewski, Acta Phys. Pol. B6, 147 (1975).
[17]W. Dietrich, A. Backlin, and C. O. Lannergard, Nucl. Phys. A253, 429 (1975).
[18]J. Rekstad and G. Løvhøiden, Nucl. Phys. A267, 40 (1976).
[19]Bibijana Cujec, Phys. Rev. 131, 735 (1963); B. L. Cohen, J. B. Moorhead, and R. A. Moyer, *ibid.* 161, 1257 (1967); B. L. Cohen, R. A. Moyer, J. B. Moorhead, L. H. Goldman, and R. C. Diehl, *ibid.* 176, 1401 (1968); R. C. Diehl, B. L. Cohen, R. A. Moyer, and L. H. Goldman, *ibid.* 180, 1210 (1969); R. C. Diehl, B. L. Cohen, R. A. Moyer, and L. H. Goldman, Phys. Rev. C 1, 2086 (1970); F. A. Rickey and P. C. Simms, Phys. Rev. Lett. 31, 404 (1973); R. E. Anderson, R. L. Bunting, J. D. Burch, S. R. Chinn, J. J. Kraushaar, R. J. Peterson, D. E. Prull, B. W. Ridley, and R. A. Ristinen, Nucl. Phys. A242, 75 (1975).
[20]P. C. Simms, F. A. Rickey, and J. R. Tesmer, Phys. Rev. Lett. 30, 710 (1973); P. C. Simms, G. J. Smith, F. A. Rickey, J. A. Gran, J. R. Tesmer, and R. M. Steffen, Phys. Rev. C 9, 684 (1974); J. A. Gran, F. A. Rickey, G. J. Smith, P. C. Simms, and J. R. Tesmer, Nucl. Phys. A229, 346 (1974); F. A. Rickey, J. A. Gran, L. E. Samuelson, and P. C. Simms, Phys. Rev. C 15, 1530 (1977).
[21]W. Klarma and J. Rekstad, Nucl. Phys. A258, 61 (1976).
[22]Y. A. Ellis, Nucl. Data Sheets 27, 1 (1979); B. Harmatz, *ibid.* 28, 3 (1979).
[23]F. S. Stephens, R. M. Diamond, J. R. Leigh, T. Krammuri, and K. Nakai, Phys. Rev. Lett. 29, 438 (1972); J. R. Leigh, K. Nakai, K. H. Maier, F. Puhlhofer, F. S. Stephens, and R. M. Diamond, Nucl. Phys. A213, 1 (1973).
[24]J. Chiba, R. S. Hayano, M. Sekimoto, H. Nakayama, and K. Nakai, J. Phys. Soc. Jpn. 43, 1109 (1977).
[25]T. Morek, H. Beuscher, B. Bochev, D. R. Haenni, R. M. Lieder, M. Muller-Veggian, A. Neskakis, and C. Mayer-Böricke, Annual Report of the Institute of Nuclear Physics at the Kernforschungsanlage, Jülich (1979) edited by C. Mayer-Böricke, p. 44 (unpublished).
[26]E. A. Henry, Nucl. Data Sheets 11, 4 (1974).
[27]R. F. Casten, G. J. Smith, M. R. Macphail, D. Breitiq, W. R. Kane, M. L. Stelts, S. F. Muhaghab, J. A. Cizewski, H. G. Borner, W. F. Davidson, and K. Schreckenbach, Phys. Rev. C 21, 65 (1980).